Monte Carlo method for kinetic chemotaxis model and its applications on traveling pulse and pattern formation

Graduate School of Simulation Studies, University of Hyogo
Shugo YASUDA

In collaboration with Benoît Perthame
Laboratoire Jacques-Louis Lions

Plan of Talk

1. General Introduction
2. Kinetic Chemotaxis Model
3. Monte Carlo Method
4. Application 1: Traveling pulse
5. Application 2: Pattern formation
6. Concluding remarks

Introduction

Run-and-Tumble Bacteria

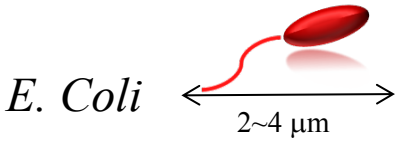

"Run": Flagella rotate counterclockwise
"Tumble": flagella rotate clockwise

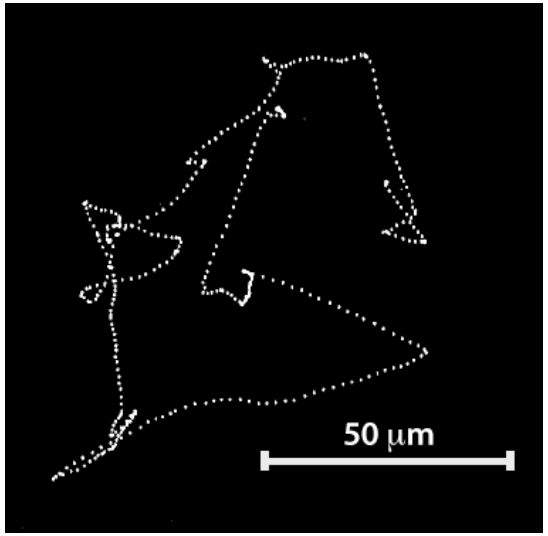

Homepage of H. C. Berg
http://www.rowland.harvard.edu/labs/bacteria/

Collective dynamics of bacteria

Pattern formation by Budrene and Berg, Nature 349, 630 (1991).

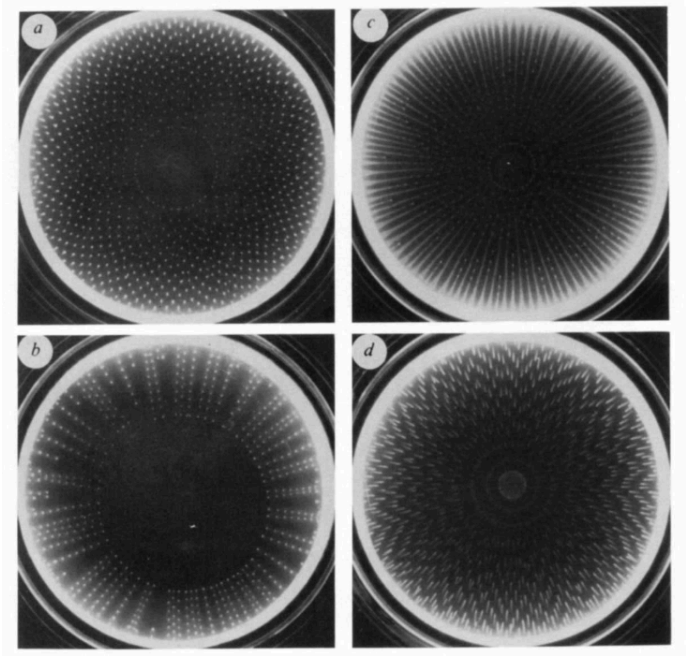

Bacteria communicate via chemical cues

Motivation

- Multiscale mechanism and mathematical hierarchy in the collective dynamics of bacteria.
  - Relation between macroscopic phenomena, individual motions, and internal states
- Simulation method
  - Extensible (modeling) and Scalable (computation)
- Applications
  - Traveling pulse, Pattern formations, ...

Objective of study

- Development of a Monte Carlo method for chemotactic bacteria based on a *kinetic chemotaxis model*.

- Applications on traveling pulse and pattern formation.
  - Validity of the MC method via comparisons to the theoretical and experimental results.
  - A new theoretical result on the instability analysis of a kinetic chemotaxis equation.

Why kinetic model?

- Mesoscopic modeling involving the individual dynamics (multiscale nature)
  - H. G. Othmer, S. R. Dunbar, and W. Alt (1988); R. Erban and H. G. Othmer (2004); Y. Dolak and C. Schmeiser (2005); N. Bellomo, A. Bellouquid, J. Nieto, and J. Soler (2007); etc..
- Mathematical hierarchy
  - T. Hillen and H. G. Othmer (2000), (2002); F. A.C.C. Chalub, P. Markowich, B. Perthame, and C. Schmeiser (2004); F. James and N. Vauchelet (2013); G. Si, M. Tang, and X. Yang (2014); B. Perthame, M. Tang, and N. Vauchelet (2016).
- Development of experimental technologies
  - J. Saragosti, V. Calvez, N. Bournaveas, B. Perthame, A. Buguin, and P. Silberzan (2011); C. Emako, C. Gayrard, A. Buguin, L. Almeida, and N. Vauchelet (2016).

Plan of Talk

1. Introduction
2. **Kinetic Chemotaxis Model**
3. Monte Carlo Simulation
4. Application 1: Traveling pulse
5. Application 2: Pattern formation
6. Concluding remarks

Schematic of kinetic modeling

Biased random motions searching for the chemical attractants

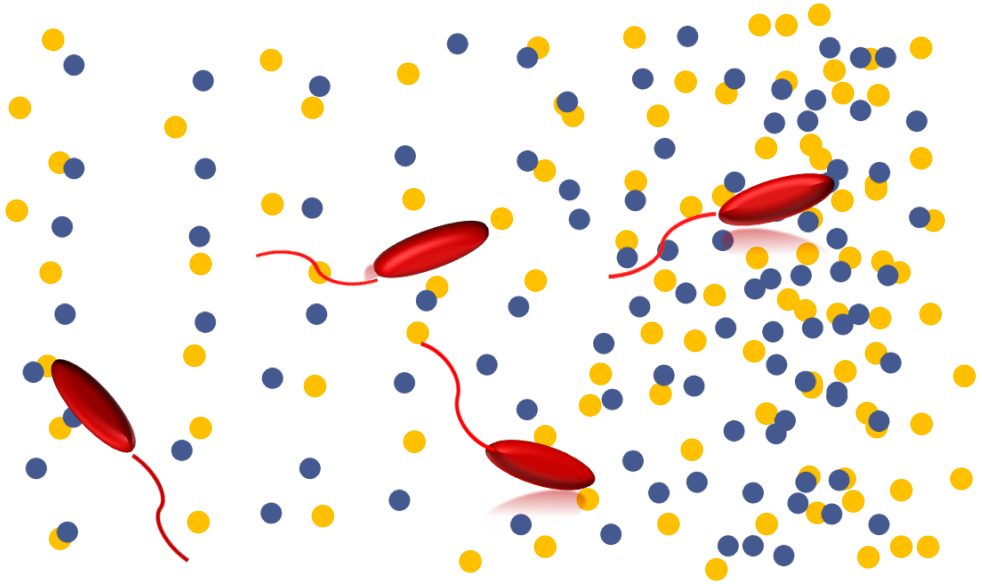

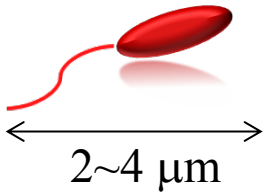

Chemical cues

- Foods
- Secretions

<< 1 μm

Schematic of kinetic modeling

Continuum description for chemical cues, $S(t, \boldsymbol{x})$

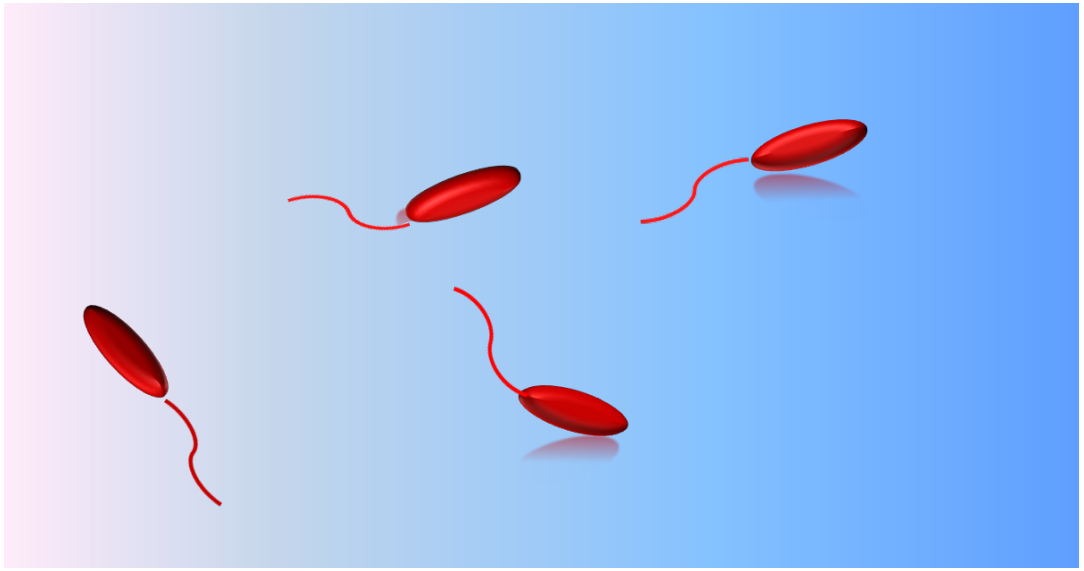

Kinetic description for bacterial density with the velocity distribution function $f(t, \boldsymbol{x}, \boldsymbol{v})$

Stiff response

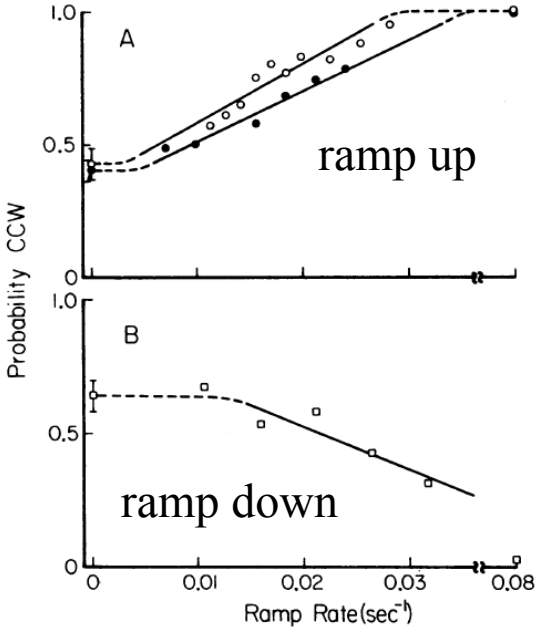

From Block SM, Segall JE, Berg HC, J. Bacteriol 154, 312 (1983)

Individual Motions of Bacteria

Run-and-Tumble motion

e.g., E-coli

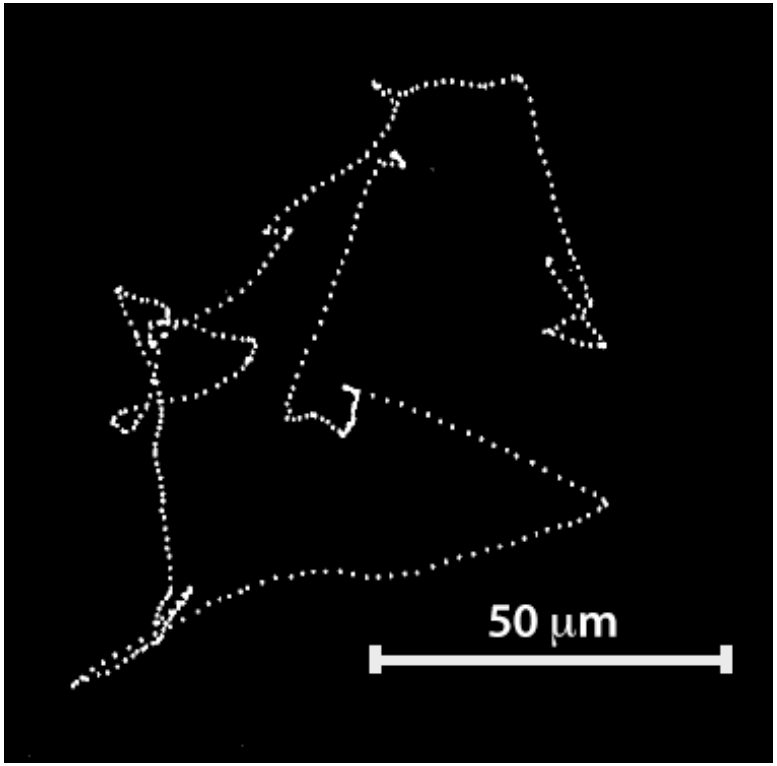

Homepage of H. C. Berg

http://www.rowland.harvard.edu/labs/bacteria/

Stochastic process

1. Tumbling at some rate λ .
2. Reorientation followed by some PDF $K(v, v')$.
3. Cell division/extinction with some rate r.

Bacterial density $f(t, x, v)$ changes during the stochastic process.

Kinetic Chemotaxis model with growth term

$$\partial_t f + v \cdot \partial_x f = \underbrace{\int T(v, v') f(t, x, v')\, dv'}_{\text{Gain Term}} - \underbrace{\int T(v', v) f(t, x, v)\, dv'}_{\text{Lost Term}} + \underbrace{r f(t, x, v)}_{\text{Cell division}}$$

Transient kernel

$$T(v, v') = \lambda(v') K(v, v')$$

$$\int K(v, v') dv = 1$$

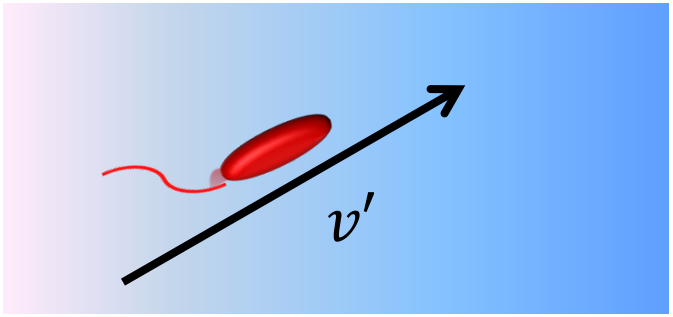

Searching for foods and chemical cues along their trajectory

Scattering Kernel

- Tumbling rate

Temporal variation along the trajectory

$$\lambda(v') = \frac{1}{2}\left[\psi_N\left(\frac{D\log N}{Dt}\bigg|_{v'}\right) + \psi_S\left(\frac{D\log S}{Dt}\bigg|_{v'}\right)\right]$$

  - Stiff response function

$$\psi(X) = \psi_0 - \chi\tanh\left(\frac{X}{\delta}\right)$$

  - Mean tumbling rate ψ_0
  - Modulation parameter $\chi_{S,N}$
  - Stiffness parameter δ^{-1}

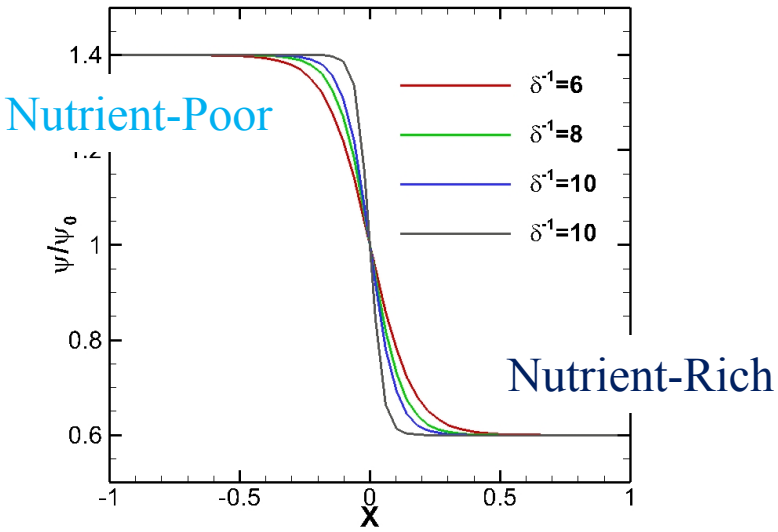

Scattering Kernel

- Reorientation (e.g., von Mises distribution)

$$K(\boldsymbol{v}, \boldsymbol{v}') = \frac{\exp\left(-\frac{1-\cos\theta}{\sigma^2}\right)}{2\pi V_0^2 \sigma^2 \left(1 - e^{-\frac{2}{\sigma^2}}\right)}$$

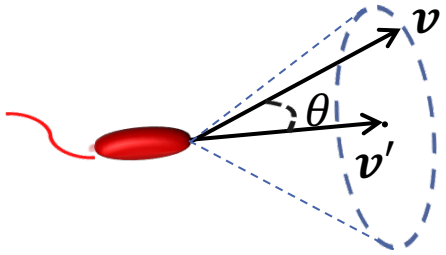

  - Reorientation angle θ
  - Constant Speed $|\boldsymbol{v}| = V_0$.
  - Standard deviation σ
    - Uniform scattering $K = \frac{1}{4\pi V_0^2}$ as $\sigma \to \infty$.

Basic equations

- Kinetic chemotaxis

$$\frac{\partial \hat{f}}{\partial \hat{t}} + \hat{e}_\alpha \frac{\partial \hat{f}}{\partial \hat{x}_\alpha} = \hat{\psi}_0 \left\{ \int_{|\boldsymbol{e}'|=1} \hat{\Psi}(\hat{\boldsymbol{e}}') \hat{K}(\hat{\boldsymbol{e}}, \hat{\boldsymbol{e}}') \hat{f}(\hat{\boldsymbol{e}}') d\Omega(\hat{\boldsymbol{e}}') - \hat{\Psi}(\hat{\boldsymbol{e}}) \hat{f}(\hat{\boldsymbol{e}}) \right\} + \hat{r} \hat{f}(\hat{\boldsymbol{e}})$$

  - Modulation of tumbling frequency, for example,

$$\hat{\Psi}(\boldsymbol{e}) = 1 - \frac{\hat{\chi}_S}{2} \tanh \left(\left. \frac{D \log \hat{S}}{\hat{\delta} D \hat{t}} \right|_{\hat{\boldsymbol{e}}} \right) - \frac{\hat{\chi}_N}{2} \tanh \left(\left. \frac{D \log \hat{N}}{\hat{\delta} D \hat{t}} \right|_{\hat{\boldsymbol{e}}} \right)$$

  - PDF of reorientation angle, for example,

$$\hat{K}(\hat{\boldsymbol{e}}, \hat{\boldsymbol{e}}') = \frac{\exp\left(\frac{1 - \hat{\boldsymbol{e}} \cdot \hat{\boldsymbol{e}}'}{\sigma^2} \right)}{2\pi\sigma^2 \left(1 - e^{-\frac{2}{\sigma^2}} \right)}$$

(von Mises distribution)

Basic equations

- Reaction-Diffusion equations of chemical cues

$$\frac{\partial \hat{S}}{\partial \hat{t}} = \hat{D}_S \frac{\partial^2 \hat{S}}{\partial \hat{x}_\alpha^2} - \hat{a}\hat{S} + \hat{b}\hat{\rho}$$

$$\frac{\partial \hat{N}}{\partial \hat{t}} = \hat{D}_N \frac{\partial^2 \hat{N}}{\partial \hat{x}_\alpha^2} - \hat{c}\hat{N}\hat{\rho} \qquad (\hat{S},\ \hat{N},\ \hat{\rho} > 0)$$

$$\hat{\rho}(\hat{t}, \hat{\boldsymbol{x}}) = \frac{1}{4\pi} \int_{|\hat{\boldsymbol{e}}'|=1} \hat{f}(\hat{t}, \hat{\boldsymbol{x}}, \hat{\boldsymbol{e}}') d\Omega(\hat{\boldsymbol{e}}')$$

Parameters

- Mean run length (or Knudsen number)

$$\hat{\psi}_0^{-1} = \frac{V_0 \psi_0^{-1}}{L_0}$$

- Stiffness and modulation in response function

$$\hat{\delta}^{-1} = \left(\frac{L_0}{V_0} \delta \right)^{-1}, \quad \hat{\chi}_{S,N} = \chi_{S,N} / \psi_0$$

- Other Parameters

$$\hat{D}_{S,N} = D_{S,N} / (L_0^2 / t_0), \quad \hat{a} = t_0 a, \quad \hat{c} = \rho_0 t_0 c, \quad \hat{r} = t_0 r$$

$$(\hat{b} = 1)$$

Plan of Talk

1. Introduction
2. Kinetic Chemotaxis Model
3. **Monte Carlo method**
4. Application 1: Traveling wave
5. Application 2: Pattern formation
6. Concluding remarks

Simulation method

- Monte Carlo method for chemotactic bacteria coupled with a finite volume scheme for chemical cues.
- Motions of bacteria calculated by MC particles.
- Macroscopic quantities are calculated based on a lattice-mesh system.
- Similar to the DSMC method for the Boltzmann equation of gases.

Lattice System and MC Particles

- Motions of bacteria by Monte Carlo particles
- Macroscopic quantities on a lattice-mesh system

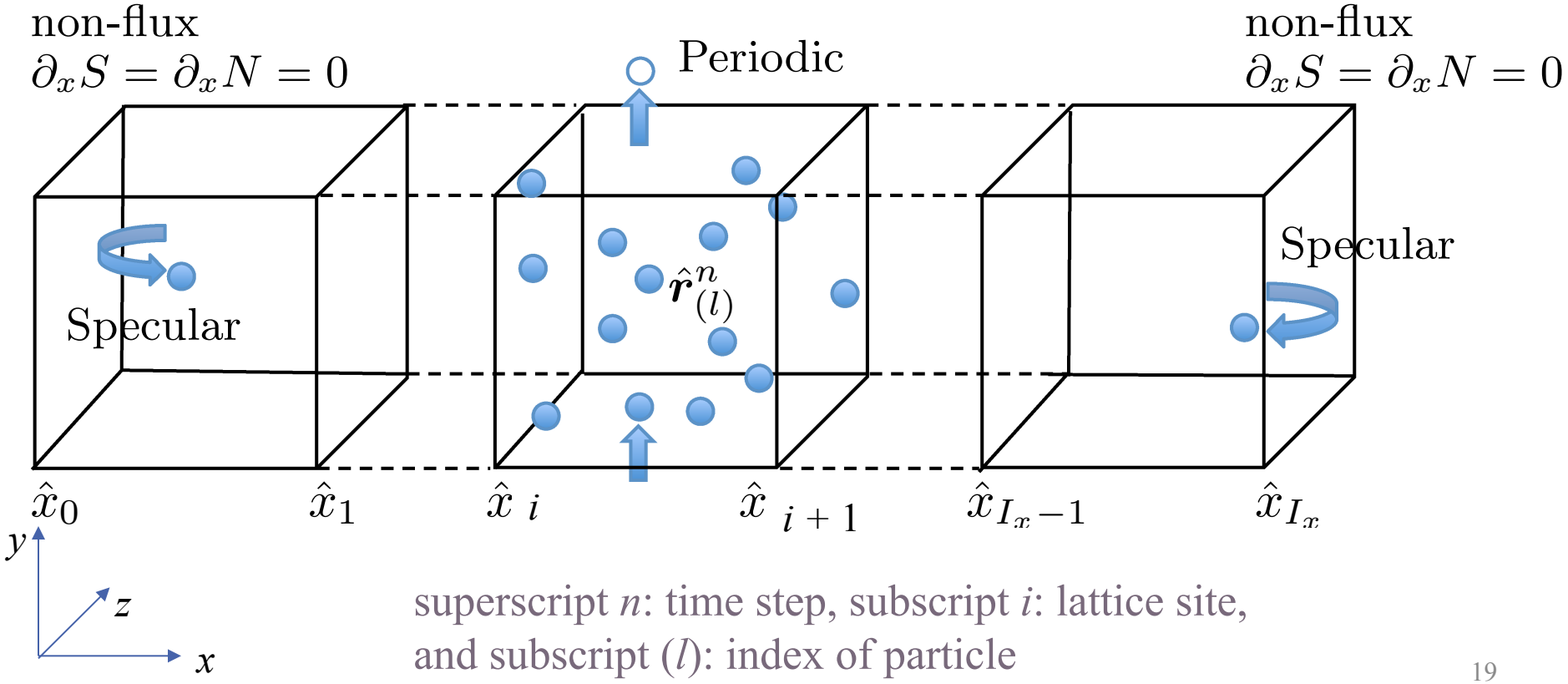

superscript n: time step, subscript i: lattice site, and subscript (l): index of particle

Calculation of Chemical Cues

- Finite volume scheme on the lattice mesh

$$\hat{F}_i^n = \hat{F}(n\Delta\hat{t}, \hat{x}_{i+\frac{1}{2}}), \quad (F = S,\ N,\ \rho)$$

$$\frac{\hat{S}_i^{n+1} - \hat{S}_i^n}{\Delta\hat{t}} = \frac{\hat{D}_S}{\Delta\hat{x}^2}\left(\hat{S}_{i+1}^n - 2\hat{S}_i^n + \hat{S}_{i-1}^n\right) - \hat{a}\hat{S}_i^{n+1} + \hat{b}\hat{\rho}_i^{n+1}$$

$$\frac{\hat{N}_i^{n+1} - \hat{N}_i^n}{\Delta\hat{t}} = \frac{\hat{D}_N}{\Delta\hat{x}^2}\left(\hat{N}_{i+1}^n - 2\hat{N}_i^n + \hat{N}_{i-1}^n\right) - \hat{c}\hat{N}_i^{n+1}\hat{\rho}_i^{n+1}$$

Population densities are calculated from the numbers of MC particles in each lattice site.

$$\hat{\rho}_i^n = \frac{1}{\Delta\hat{x}^3}\int_{i\text{th site}}\int_{\text{all}\hat{\boldsymbol{e}}'} \hat{f}(n\Delta\hat{t}, \hat{\boldsymbol{x}}, \hat{\boldsymbol{e}}')d\Omega(\hat{\boldsymbol{e}}')d\hat{\boldsymbol{x}}$$

Monte Carlo Method

0. Initialization: Distribute particles according to $\hat{f}_i{}^0(\hat{\boldsymbol{e}})$.
1. Move particles in a time-step size Δt.
2. Calculation of local concentration of chemical cues.
3. Tumbling of each particle by a probability $\hat{\lambda}(\hat{\boldsymbol{e}}'_{(l)})\Delta\hat{t}$.
4. Reorientation angle by $K(\hat{\boldsymbol{e}}, \hat{\boldsymbol{e}}')$.
5. Division by a probalibity $\hat{r}\Delta\hat{t}$.
6. Return to 1.

Monte Carlo Method

0. Initialization:

MC particles are distributed according to $\hat{f}_i^0(\hat{\boldsymbol{e}})$.

- Calculate particle number in the i th lattice site μ_i^0 via

$$(L_0 \Delta \hat{x})^3 \rho_0 \hat{\rho}_i = w_0 \mu_i$$

- where w_0 is the uniform weight of a single MC particle
- In each lattice site, particles are randomly distributed.
- Velocity of particle is determined by the PDF $\hat{f}_i^0(\hat{e})/\hat{\rho}_i^0$

Monte Carlo Method

1. Movement: Particles move with their velocities in a time step size Δt.

$\hat{\boldsymbol{r}}_{(l)}$, $\hat{\boldsymbol{e}}_{(l)}$: position and velocity of l th particle

$$\hat{\boldsymbol{r}}_{(l)}^{n+1} = \hat{\boldsymbol{r}}_{(l)}^{n} + \hat{\boldsymbol{e}}_{(l)}^{n}\Delta\hat{t} \quad (l = 1, \cdots, M^n)$$

- Particles beyond the boundaries are removed and new ones are inserted following the boundary conditions.

- Count the numbers of simulation particles in each lattice site ${\mu_i}^{n+1}$ $(i = 0, \ldots, I_x - 1)$.

Monte Carlo Method

2. Calculation of chemical cues at each lattice site.
   - with $\hat{\rho}_i^{n+1} = w_0 {\mu_i}^{n+1}/[(L_0\Delta x)^3\rho_0]$.

$$\frac{\hat{S}_i^{n+1} - \hat{S}_i^n}{\Delta\hat{t}} = \frac{\hat{D}_S}{\Delta\hat{x}^2}\left(\hat{S}_{i+1}^n - 2\hat{S}_i^n + \hat{S}_{i-1}^n\right) - \hat{a}\hat{S}_i^{n+1} + \hat{b}\hat{\rho}_i^{n+1}$$

$$\frac{\hat{N}_i^{n+1} - \hat{N}_i^n}{\Delta\hat{t}} = \frac{\hat{D}_N}{\Delta\hat{x}^2}\left(\hat{N}_{i+1}^n - 2\hat{N}_i^n + \hat{N}_{i-1}^n\right) - \hat{c}\hat{N}_i^{n+1}\hat{\rho}_i^{n+1}$$

Monte Carlo Method

3. Tumbling of the l th particle by a probability $(\hat{\psi}_0 \Delta\hat{t})\hat{\Psi}(\hat{\boldsymbol{e}}_{(l)}^n)$,

$$\hat{\Psi}(\hat{\boldsymbol{e}}_{(l)}^n) = 1 - \frac{\hat{\chi}_S}{2}\tanh\left(\frac{\log \hat{S}_{(l)}^{n+1}/\hat{S}_{(l)}^n}{\hat{\delta}\Delta\hat{t}}\right) - \frac{\hat{\chi}_N}{2}\tanh\left(\frac{\log \hat{N}_{(l)}^{n+1}/\hat{N}_{(l)}^n}{\hat{\delta}\Delta\hat{t}}\right)$$

$$\left.\frac{D\log N}{Dt}\right|_{\boldsymbol{e}} \Rightarrow \frac{\log N_{(l)}^{n+1} - \log N_{(l)}^n}{\Delta t}$$

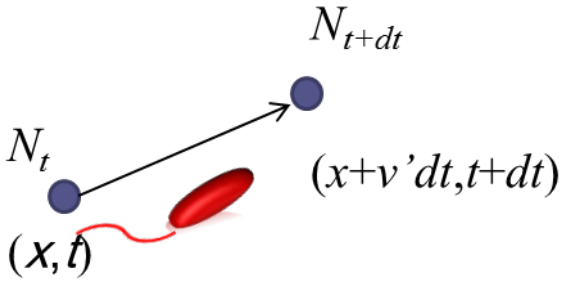

Temporal variation along the pathway $\hat{\boldsymbol{r}}_{(l)}^n \rightarrow \hat{\boldsymbol{r}}_{(l)}^{n+1}$.

Monte Carlo Method

3. Tumbling of the lth particle by a probability $\left(\hat{\psi}_0 \Delta\hat{t}\right)\hat{\Psi}(\hat{\boldsymbol{e}}^n_{(l)})$,
   - $\hat{S}^n_{(l)}, \hat{N}^n_{(l)}$: sensed by the lth MC particle at $\hat{\boldsymbol{r}}^n_{(l)}$
   - Calculated by the interpolation, $\hat{r}_{x(l)} \in [\hat{x}_i, \hat{x}_{i+1}]$

$$\hat{F}_{(l)} = \hat{F}_i + \frac{\hat{F}_{i+1} - \hat{F}_{i-1}}{2\Delta x}\left(\hat{r}_{x(l)} - \hat{x}_{i+\frac{1}{2}}\right)$$

   - The particles that stay at the same lattice site after Δt passes can sense the gradients.

Monte Carlo Method

4. Reorientation angle by a probability $\widehat{K}(\hat{\boldsymbol{e}}_{(l)}^{n+1}, \hat{\boldsymbol{e}}_{(l)}^{n})$.

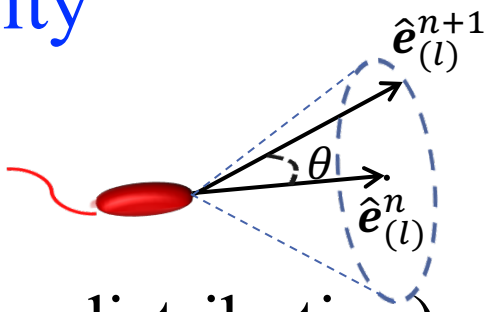

   - Reorientation angle θ (for von Mises distribution)

$$\cos\theta = 1 + \sigma^2 \log\left[e^{-\frac{2}{\sigma^2}} + \left(1 - e^{-\frac{2}{\sigma^2}}\right) U_1\right]$$

5. Cell divisions (or deaths) with a probability $\hat{r}\Delta\hat{t}$.
6. Return to step 1 (Movement Step).

Monte Carlo Method

- First order accuracy in time and space under the assumption of the law of large numbers.
  - B. Perthame and S. Yasuda, “Self-organized pattern formation of run-and-tumble chemotactic bacteria: Instability analysis of a kinetic chemotaxis model”, hal-01494963 (2017).

Plan of Talk

1. Introduction
2. Kinetic Chemotaxis Model
3. Monte Carlo Simulation
4. Application 1: Traveling pulse
5. Application 2: Pattern formation
6. Concluding remarks

- # Literature on traveling pulse

by J. Saragosti, V. Calvez, N. Bournaveas, B. Perthame, A. Buguinn, and P. Silberzan, PNAS 108, 16235(2011)

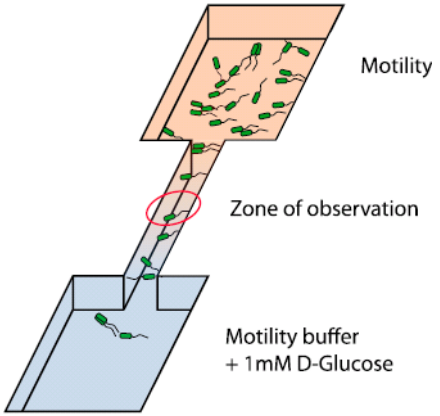

V_{wave}=4.1 μm/s

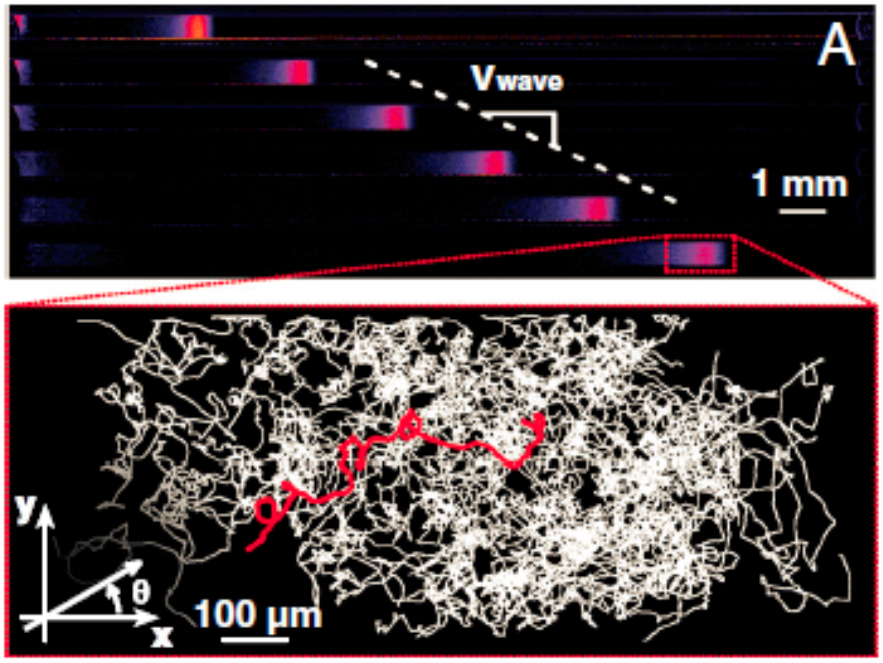

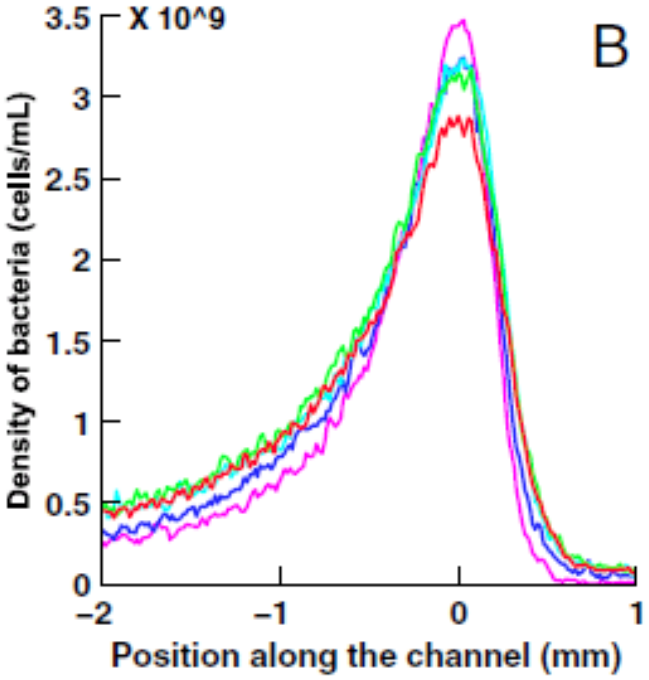

Problem and parameter setting

- Initial condition and geometry

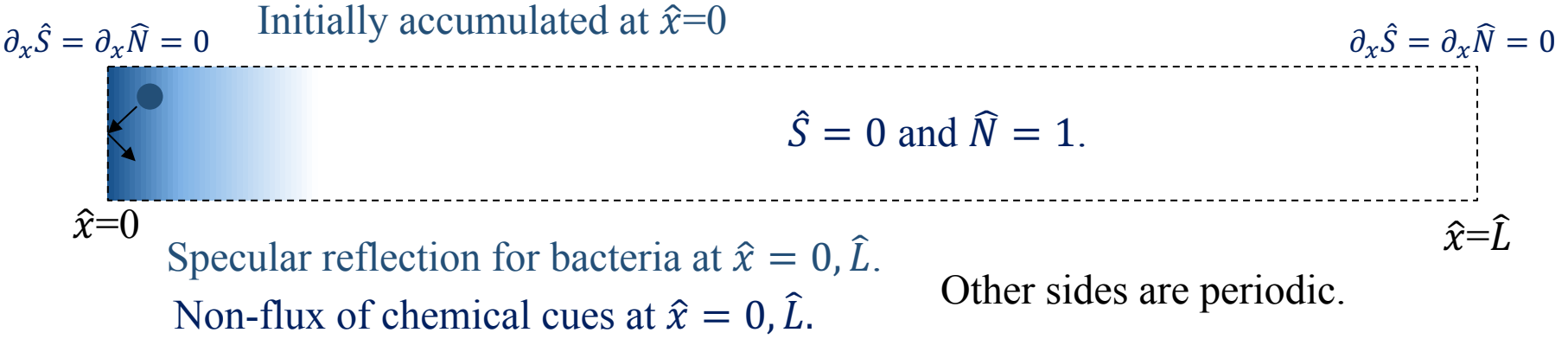

- Parameter setting
  - Mean tumbling frequency $\psi_0 = 3.0$ [1/s] $(\hat{\psi}_0^{-1} = 0.00833)$
  - Modulation of the response $\hat{\chi}_S = 0.2$ and $\hat{\chi}_N = 0.6$.
  - Stiffness of the response $\delta = 0.125$ [1/s].
  - Division rate $\hat{r} = 0.0067$.
  - Chanel length $\hat{L} = 18$.
  - Total particle number 56640.
  - $\Delta\hat{x} = 0.025, \Delta\hat{t} = 0.005$. $(\Delta\hat{t} < \hat{\psi}_0^{-1})$

J. Saragosti, V. Calvez, N. Bournaveas, B. Perthame, A. Buguin, and P. Silberzan, PNAS 108, 16235(2011)

Movie on the bacterial motions

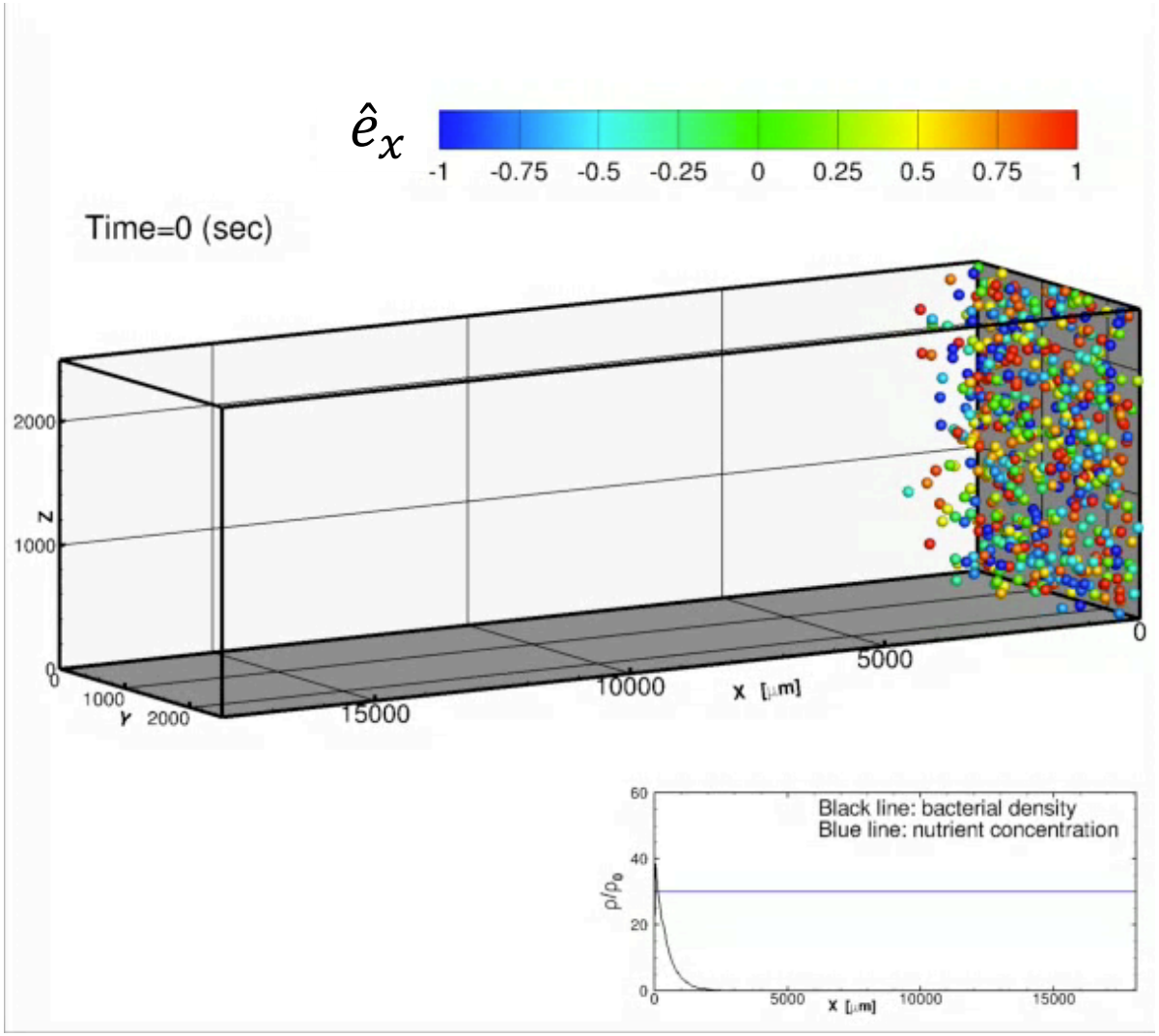

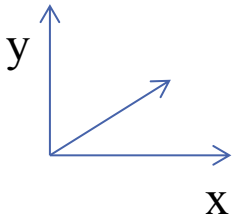

Boundary condition
Specular for x and
periodic for y and z.

Application to the traveling wave

Time progress of population density

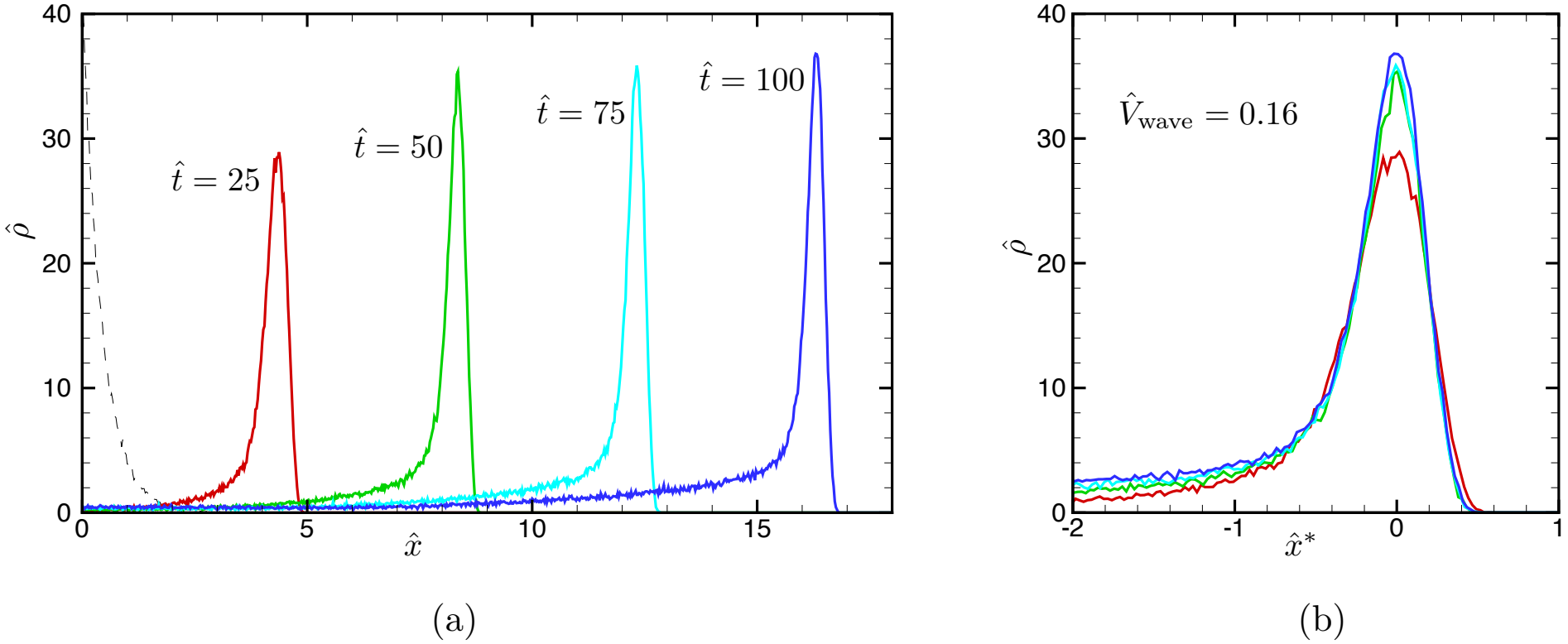

(a) (b)

Fig1. Time progress of population density of bacteria along the channel. (a) the snap shots and (b) super position of the density profiles in the moving frame $\hat{x}^*$ with a constant wave velocity V_{wave}**=4.0 μm/s**. (In experiment V_{wave}**=4.1 μm/s**.)

Comparison to the asymptotic analysis

- Diffusion scaling, a new reference time t'_0

$$\varepsilon = \hat{\psi}_0^{-1}$$

$$t'_0 = t_0/\varepsilon \left(= \psi_0 L_0^2/V_0^2\right)$$

- Small modulation and small division rate

$$\hat{\chi}_{S,N} = \varepsilon \phi_{S,N}$$

$$\hat{r} = \varepsilon r$$

Diffusion limit

Keller-Segel type

Chemotaxis **Random walk** **Proliferation**

$$\partial_t \rho_0 + \partial_\alpha \left(u_\alpha[S, N] \rho_0 \right) = \frac{1}{3} \Delta \rho_0 + r[\rho_0] \rho_0$$

$$u_\alpha[S, N] = \sum_{F=S,N} \frac{\phi_F}{2} \frac{\nabla \log F}{|\nabla \log F|} I[|\nabla \log F|]$$

$$I[|\nabla \log F|] = \int_0^1 \zeta \tanh(\delta^{-1} |\nabla \log F| \zeta) d\zeta$$

Comparison of Kinetic and Continuum

- Non-proliferation
  - $r = 0$
- Tumbling frequency
  - $\varepsilon = 0.02, 0.013, 0.01, 0.005,$ and 0.001
- Other Parameter
  - $\phi_N = 72, \phi_S = 24, \delta^{-1} = 0.2,$
  - $a = 24, c = 120, D_s = D_N = 3.84$

MC vs. Continuum

- Snapshot of Population density

No proliferation r=0

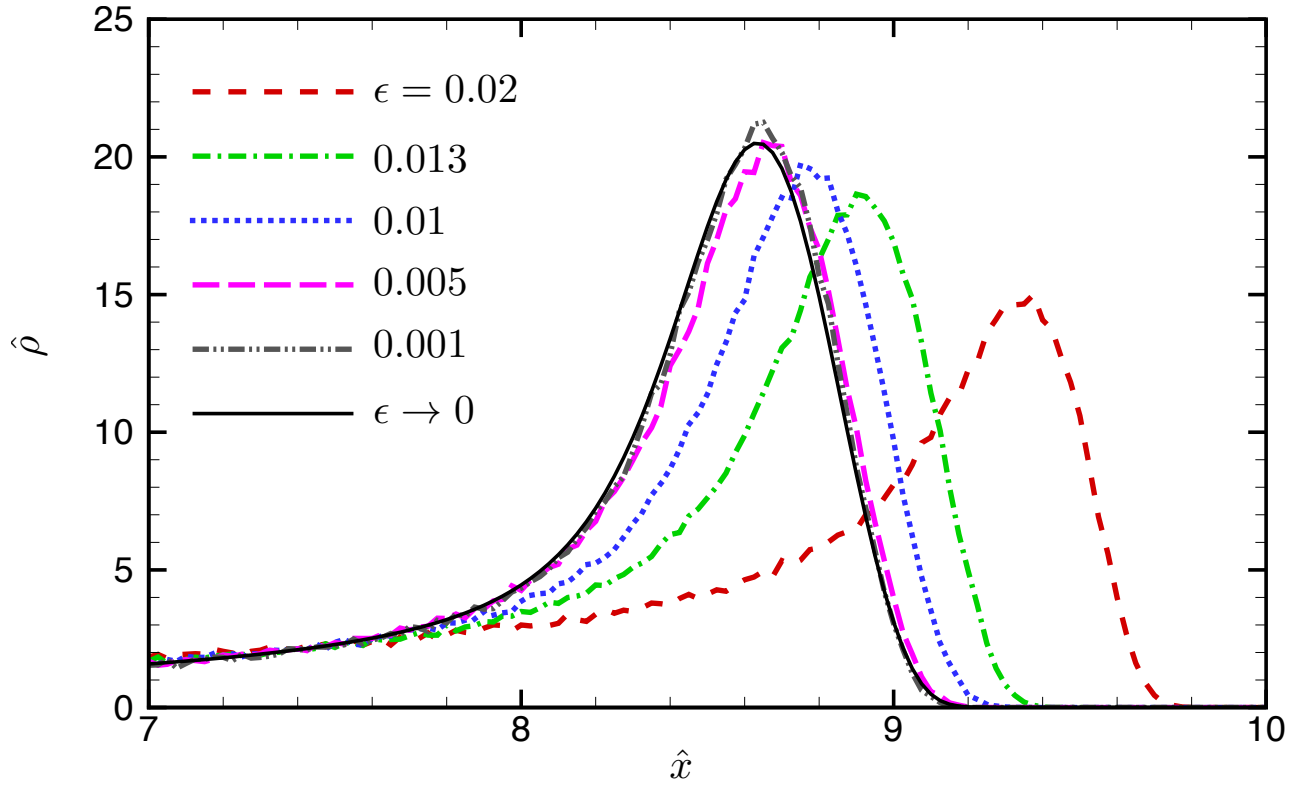

Fig. 1 Comparison of the snapshots of population density of bacteria at t=0.5 between various Knudsen numbers.

MC vs. Continuum

- Traveling speed

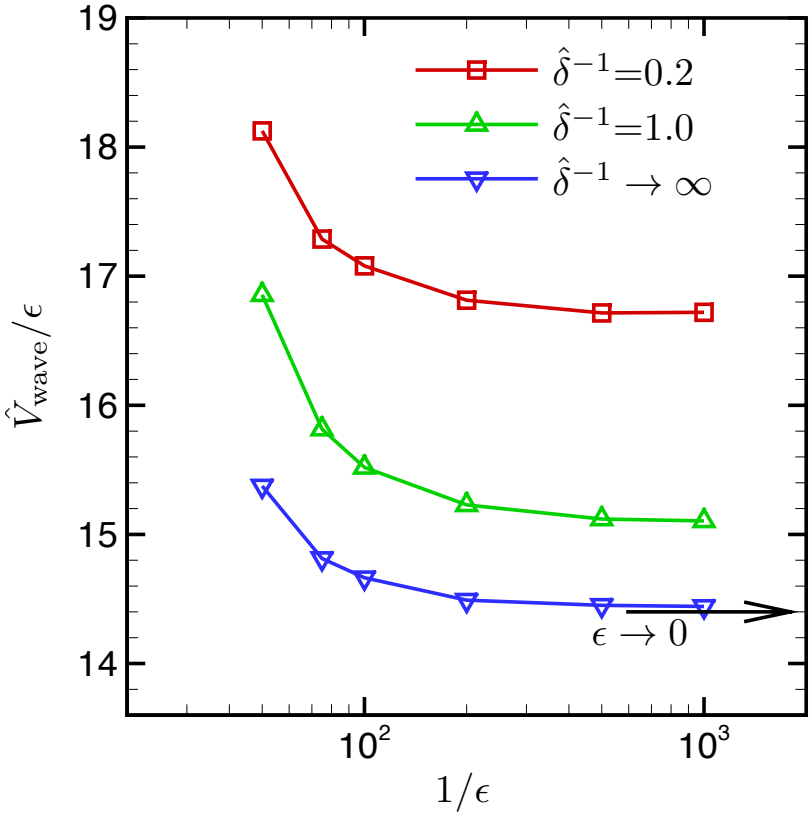

Fig. 2 The convergence of the traveling speed in the continuum limit. The right-arrow shows the result of the analytic formula obtained for the sign response function in the continuum limit (PLoS Comput. Biol. 6, e1000890 (2010)).

Effect of the stiffness and modulation

- Population density profile

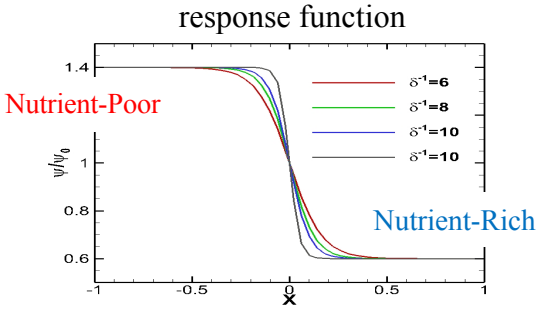

Variation in stiffness $\hat{\delta}^{-1}$

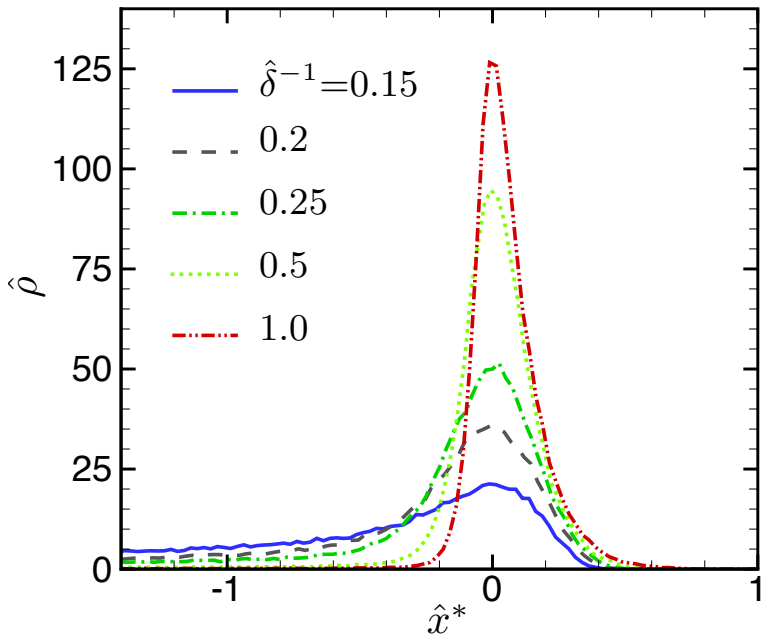

(a)

Variation in modulation $\hat{\chi}_N$

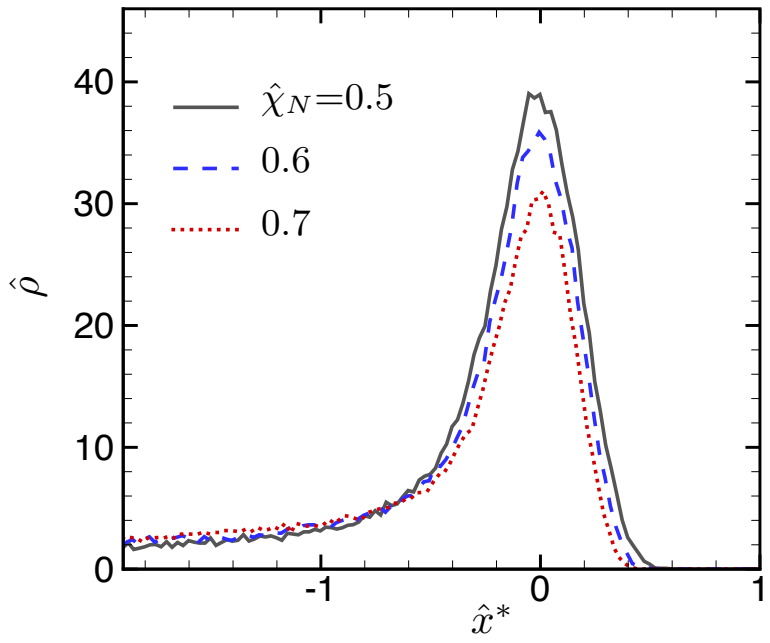

(b)

Fig. 4 The effect of the variations in stiffness and modulation parameters on the population density profile in the moving frame $\hat{x}^*$.

Effect of the stiffness and modulation

- Traveling speed

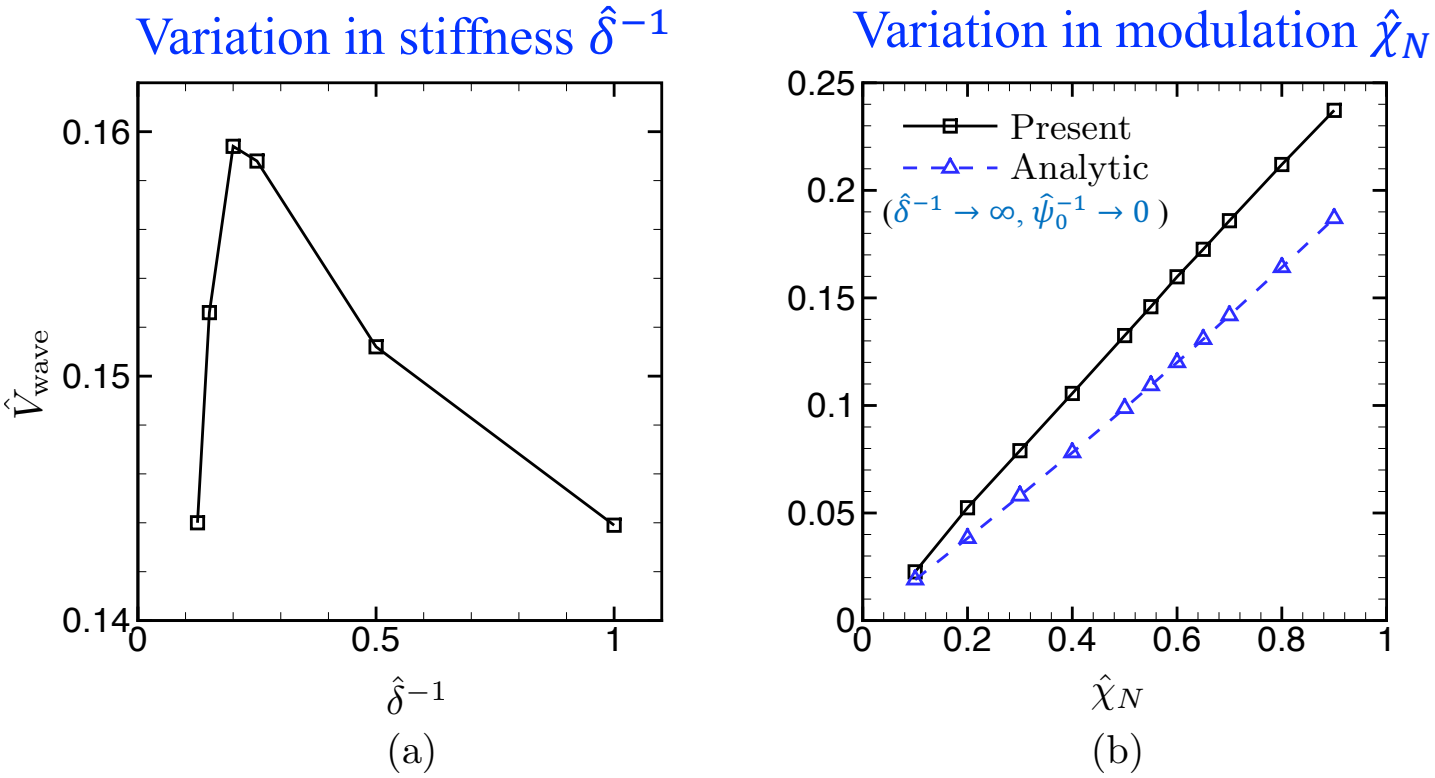

Fig. 5 The effect of the variations in stiffness and modulation parameters on the traveling speed. The analytic formula is obtained for the sign response function in the continuum limit (PLoS Comput. Biol. 6, e1000890 (2010)).

Effect of the stiffness and modulation

- Velocity distribution at the peak of the wave

Variation in stiffness $\hat{\delta}^{-1}$

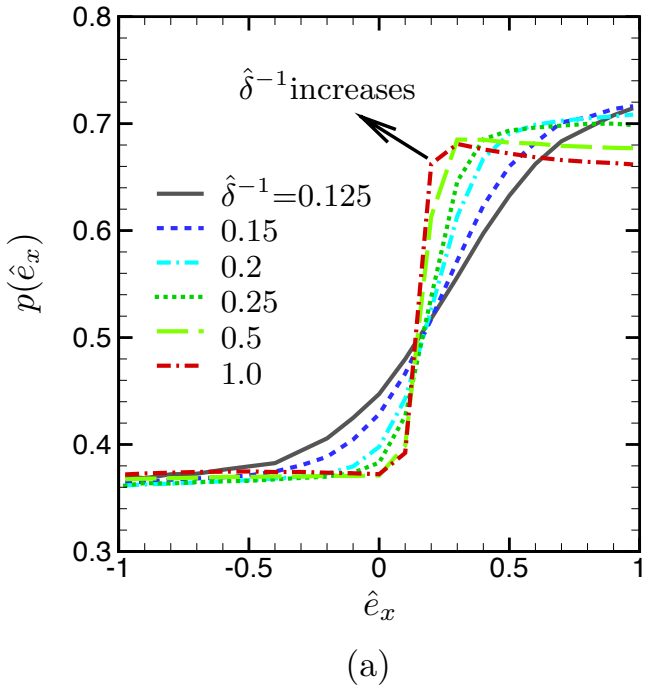

(a)

Variation in modulation $\hat{\chi}_N$

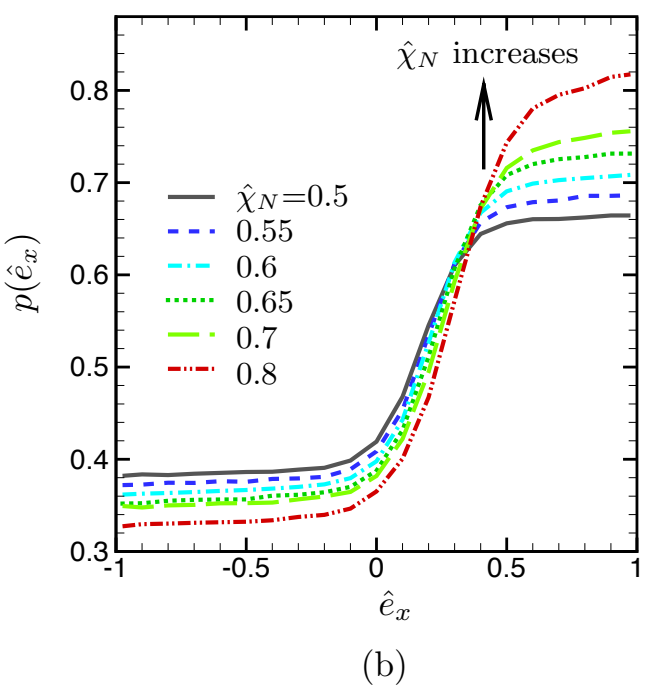

(b)

Fig. 7 The effect of the variations in stiffness and modulation parameters on the PDF of the velocity at the peak of the wave $\hat{x}^* = 0$.

Remarks on application 1

- Reproduce the experimental result.
- Recover the Keller-Segel equation in the continuum limit.
- Importance of the kinetic model for a small (but finite) value of ε.
- An orthogonal effect of the stiffness δ and modulation χ on the profile of population density and traveling speed.

Plan of Talk

1. Introduction
2. Kinetic Chemotaxis Model
3. Monte Carlo Simulation
4. Application 1: Traveling pulse
5. Application 2: Pattern formation
6. Concluding remarks

Basic equation

- Kinetic chemotaxis model with a population growth term

$$\partial_t f(t,\boldsymbol{x},\boldsymbol{v}) + \boldsymbol{v}\cdot\nabla f = \frac{1}{k}\left\{\frac{1}{4\pi}\int_V K[D_t \log S|_{\boldsymbol{v}'}] f(\boldsymbol{v}')d\Omega(\boldsymbol{v}') - K[D_t \log S|_{\boldsymbol{v}}] f(\boldsymbol{v})\right\} + P[\rho] f(\boldsymbol{v})$$

$$t \geq 0, \quad \boldsymbol{x} \in \mathbb{R}, \quad \boldsymbol{v} \in V \subset \mathbb{R} : |\boldsymbol{v}| = 1$$

- Only one chemical attractant

$$-d\Delta S(t,\boldsymbol{x}) + S(t,\boldsymbol{x}) = \rho(t,\boldsymbol{x})$$

- Biased Tumbling, Uniform scattering
  - $K[X] = 1 - F[X]$,
  - $F[0] = 0, F'[0] > 0.$

Basic equation

- Growth term $P[\rho]$: Saturated at $\rho = 1$

$$P[0] = 1,$$
$$P[\rho] > 0, \text{ for } 0 < \rho < 1, \quad (\text{ Division at the rate } P[\rho])$$
$$P[\rho] < 0, \text{ for } \rho > 1, \quad (\text{Extinction at the rate } |P[\rho]|)$$
$$P[\rho] \simeq 1 - \rho, \text{ for } \rho \simeq 1.$$

- Stationary uniform solution

$$f(t, \boldsymbol{x}, \boldsymbol{v}) = S(t, \boldsymbol{x}) = \rho(t, \boldsymbol{x}) = 1$$

Linear instability Condition

- The uniform solution is linearly unstable if the stiffness of the response function $F'[0]$ is sufficiently large as

$$\frac{F'[0]}{k} > \inf_{\lambda} \left[1 + \frac{k}{\frac{k\lambda}{\arctan(k\lambda)} - 1} \right] (1 + d\lambda^2)$$

- In addition, the unstable eigenmodes are bounded and no high frequency oscillations exist.

B. Perthame & S. Yasuda, "self-organized pattern formation of run-and-tumble chemotactic bacteria: Instability analysis of a kinetic chemotaxis model", hal-01494963 (2017).

Linear instability analysis

- Perturbation around the uniform state,

$$f(t,\boldsymbol{x},\boldsymbol{v}) = 1 + g(\boldsymbol{x},\boldsymbol{v})e^{\mu t}, \quad S(t,\boldsymbol{x}) = 1 + S_g(\boldsymbol{x})e^{\mu t}, \quad \rho(t,\boldsymbol{x}) = 1 + \rho_g(\boldsymbol{x})e^{\mu t},$$

- Fourier transform on $\boldsymbol{x}$ and Moment on $\boldsymbol{v}$,

$\boldsymbol{\lambda}$: wave vector

$$\hat{g}(\boldsymbol{\lambda},\boldsymbol{v}) = \frac{1 - k + \mathrm{i}\frac{F'[0]}{1+d\lambda^2}\boldsymbol{\lambda}\cdot\boldsymbol{v}}{1 + k\mu + \mathrm{i}\boldsymbol{\lambda}\cdot\boldsymbol{v}}\hat{\rho}_g(\boldsymbol{\lambda})$$

$$\hat{\rho}(\boldsymbol{\lambda}) = \frac{1}{2}\int_{-1}^{1} \frac{\left(1 - k + \mathrm{i}\frac{F'[0]\lambda v}{1+d\lambda^2}\right)\left(1 + k\mu_1 - \mathrm{i}k\lambda(\mu_2 + v)\right))}{(1 + k\mu_1)^2 + k^2\lambda^2(\mu_2 + v)^2} dv\hat{\rho}_g(\boldsymbol{\lambda})$$

$$\mu_1 = \mathrm{Re}(\mu), \quad \mu_2 = \mathrm{Im}(\mu)/\lambda$$

Linear instability analysis

- For non-trivial solution $\hat{\rho}_g$;

$$\left(\alpha - \frac{\beta}{\xi}\right)\left[\arctan(\xi(\mu_2+1)) - \arctan(\xi(\mu_2-1))\right] - \mu_2\beta \log\left(1 + \frac{4\mu_2}{\xi^{-2} + (\mu_2-1)^2}\right) = 2 - 2\beta$$

$$\mu_2\beta\left[\arctan(\xi(\mu_2+1)) - \arctan(\xi(\mu_2-1))\right] + \frac{1}{2}\left(\alpha - \frac{\beta}{\xi}\right)\log\left(1 + \frac{4\mu_2}{\xi^{-2} + (\mu_2-1)^2}\right) = 0$$

$$\alpha = \frac{1-k}{k\lambda}, \quad \beta = \frac{F'[0]}{k(1+d\lambda^2)}, \quad \xi = \frac{k\lambda}{1+k\mu_1}$$

- No solutions at $\lambda \to \infty$ for the first equation.
- $\mu_2 = 0$ always satisfies the second equation.

Linear instability analysis

- No solutions at $\lambda \to \infty$ for the first equation.

$$\left(\alpha - \frac{\beta}{\xi}\right)\left[\arctan(\xi(\mu_2+1)) - \arctan(\xi(\mu_2-1))\right] + \mu_2\beta\log\left(\frac{\xi^{-2}+(\mu_2-1)^2}{\xi^{-2}+(\mu_2+1)^2}\right) = 2-2\beta$$

$$\alpha = \frac{1-k}{k\lambda}, \quad \beta = \frac{F'[0]}{k(1+d\lambda^2)}, \quad \xi = \frac{k\lambda}{1+k\mu_1}$$

- The RHS converges to 2 and the second term of LHS is always non-positive.
- The first term of LHS converges to zero.
  - When ξ converges to a finite value or diverges, this is obvious because $\alpha, \beta \to 0$.
  - When $\xi \to 0$,

$$\begin{aligned}\left|\arctan(\xi(\mu_2+1)) - \arctan(\xi(\mu_2-1))\right| &= \left|\arctan\left(\frac{2\xi}{1+\xi^2(\mu_2^2-1)}\right)\right| \\ &< \left|\arctan\left(\frac{2\xi}{1-\xi^2}\right)\right| = |2\xi + \mathcal{O}(\xi^2)|\end{aligned}$$

- **No eigenmodes exist in the large-oscillation limit.**

Linear instability analysis

- Under an assumption $\mu_2 = 0$.

$$(\alpha\xi - \beta)\frac{\arctan(\xi)}{\xi} = 1 - \beta$$

  - $\mu_1 = \frac{\lambda}{\xi} - \frac{1}{k} > 0 \leftrightarrow 0 < \xi < kl.$

- Instability condition

$$\frac{F'[0]}{k} > \left[1 + \frac{k}{\frac{k\lambda}{\arctan(k\lambda)} - 1}\right](1 + d\lambda^2)$$

Kinetic Instability Diagram

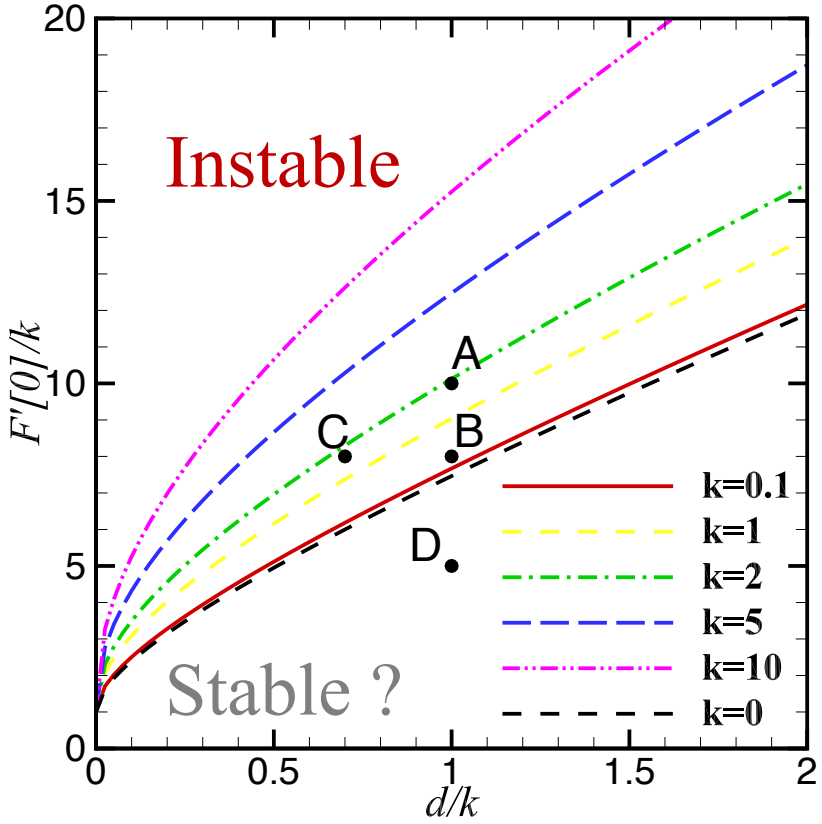

Kinetic Instability Diagram. *Chemotaxis-induced* instability takes place when the parameter value of $(\frac{F'[0]}{k}, \frac{d}{k})$ exceeds the critical line for each value of k.

Monte Carlo results

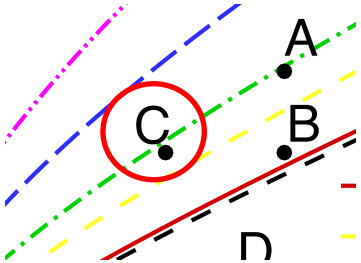

Slightly above the critical line (yellow)

$k = 1$

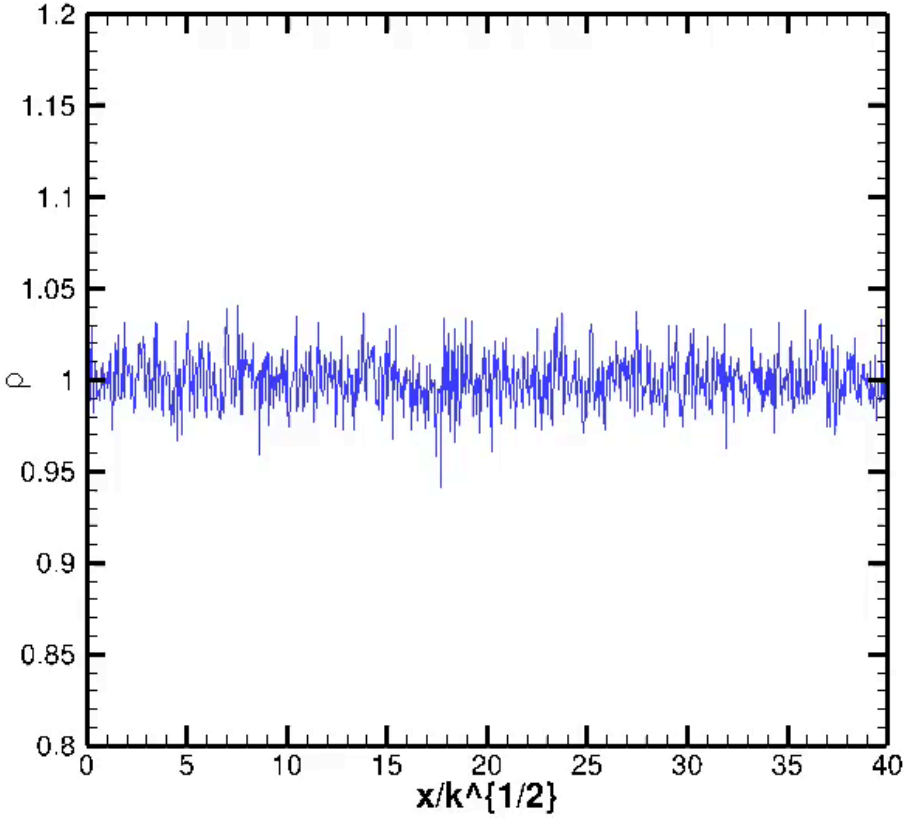

Monte Carlo results

$k = 2$

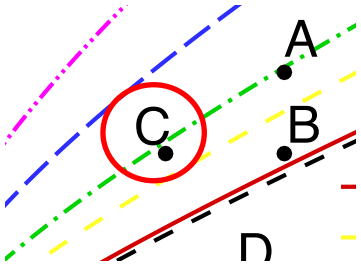

Slightly below the critical line (green)

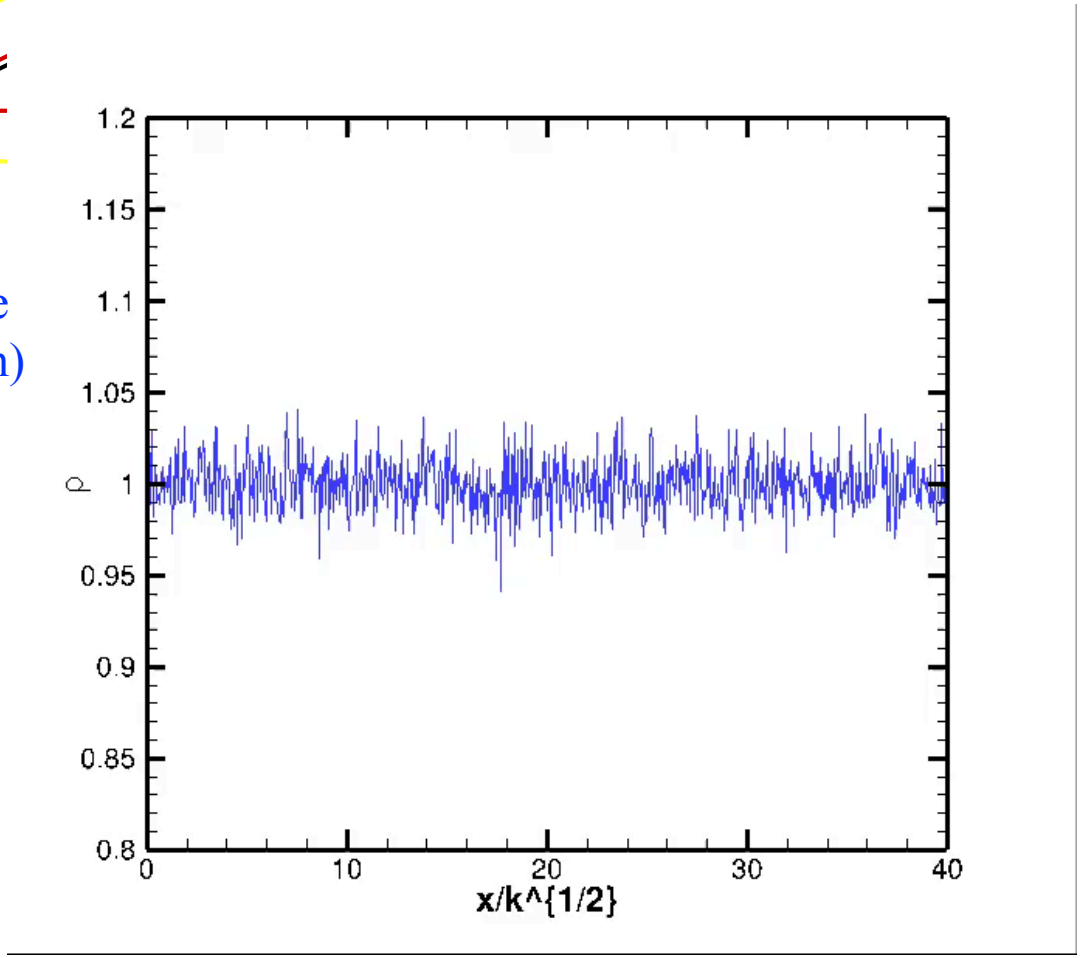

Monte Carlo results

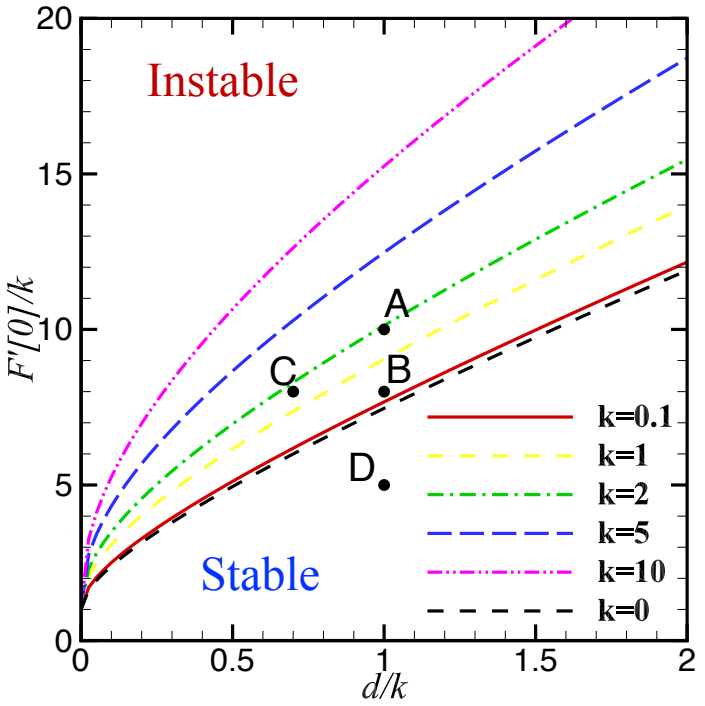

Stationary periodic

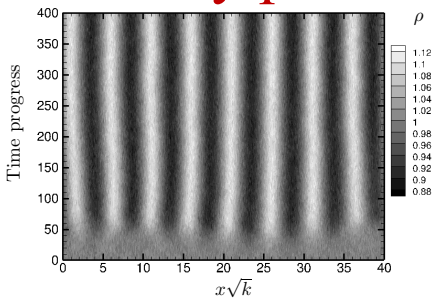

(a)

No patterns

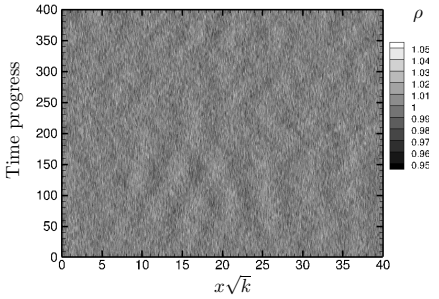

(b)

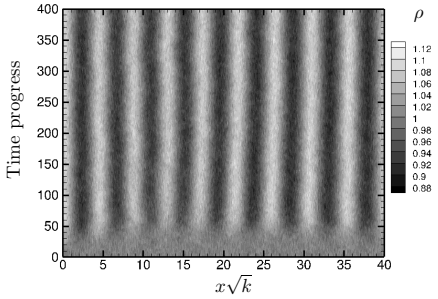

(c)

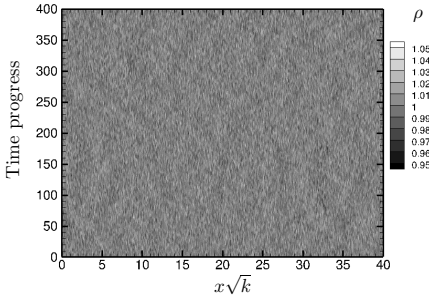

(d)

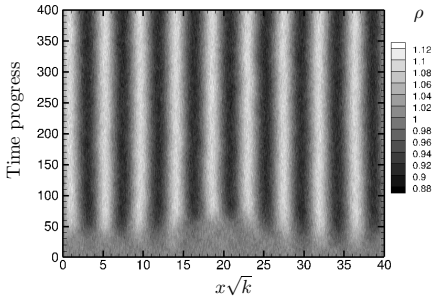

(e)

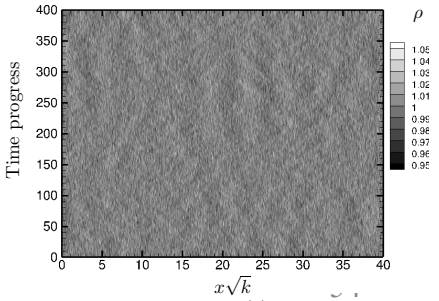

(f)

Monte Carlo results

Power spectra of population density

Periodic patterns

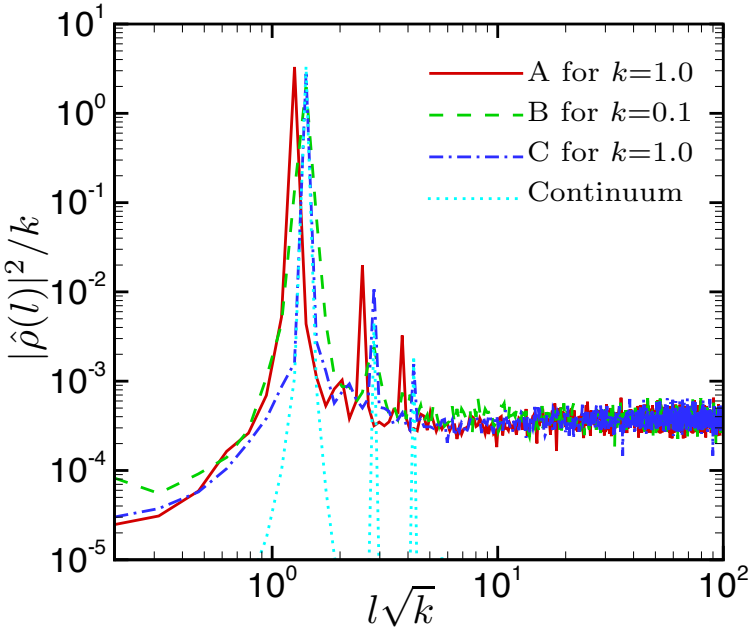

(a)

No patterns

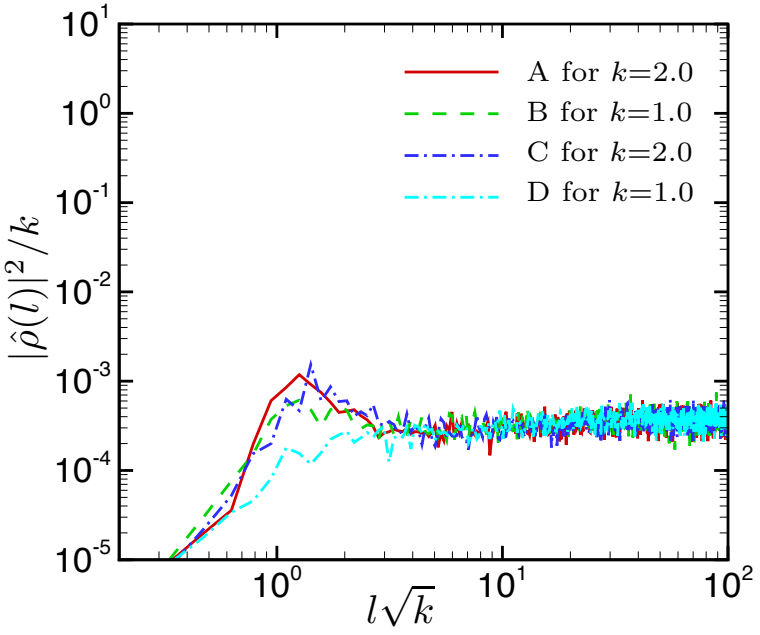

(b)

- The unstable frequencies remain bounded as in the Turing instability.
- Neither growth nor damping at high oscillations in the kinetic results.

Concluding remarks

- A Monte Carlo method for run-and-tumble chemotactic bacteria.
- *Chemotaxis-induced* instability condition in a kinetic chemotaxis equation with growth term.
- The validity of the MC method is strengthened via the comparison with the experimental (from a literature) and theoretical results.
- Future works
  - Applications; Traveling waves, 2D pattern
  - Development; Internal states (or Memories)

Thank you very much

Acknowledgements
Financial supports: IHP RIP program, CNRS, and JSPS

References

[1] S. Yasuda, “Monte Carlo simulation for kinetic chemotaxis model: An application to the traveling population wave”, J. Comput. Phys. 330, 1022–1042 (2017).
[2] B. Perthame and S. Yasuda, “Self-organized pattern formation of run-and-tumble chemotactic bacteria: Instability analysis of a kinetic chemotaxis model”, hal-01494963 (2017).